Journal of Applied Electrochemistry **34**: 601–605, 2004.
© 2004 *Kluwer Academic Publishers. Printed in the Netherlands.*

Voltammetric and morphological characterization of heteropolyanions and copper co-electrodeposition by *in situ* AFM

T. HERNÁNDEZ-PÉREZ[1], S. HOLGUÍN[1] and M. RIVERA[2,*]
[1]*Dpto. de C. Básicas, Area de Química. Universidad Autónoma Metropolitana-Azcapotzalco, Av. San. Pablo 180, 02200, México D.F., México*
[2]*Instituto de Química, UNAM. Circuito exterior, CU, 04510, México D.F., México*
*(*author for correspondence, fax: +52 (55) 5616 2203), e-mail: mrivera@servidor.unam.mx)*

Received 13 March 2003; accepted in revised form 1 December 2003

Key words: cobalt, co-electrodeposition, copper, heteropolyanion, *in situ* AFM, rhodium

Abstract

The electrodeposition of three different heteropolyoxometalates: (HPOM) $(NH_4)_3[RhMo_6O_{18}(OH)_6] \cdot 7\ H_2O$, HPOM (**1**), Cu(II)$(NH_4)[RhMo_6O_{18}(OH)_6] \cdot 7\ H_2O$, HPOM (**2**) and Cu(II)$NH_4\ [CoMo_6O_{18}(OH)_6] \cdot 7\ H_2O$ HPOM (**3**) was studied by *in situ* atomic force microscopy (AFM) and cyclic voltammetry. It was found that the voltammetric response of compounds **2** and **3** show the deposition of the copper countercation as well as the simultaneous reduction of the corresponding heteropolyanion (HPA). AFM was used to monitor the *in situ* film formation of the electroreduced species on the working electrode surface. The AFM images show important differences in the film texture when copper is present in the complex.

1. Introduction

Heteropolyanions, $[X_xM_mO_y]^{p-}$ $(x \leqslant m)$ (where M represents Mo, W, V and X represents P, Si, As) have received attention in material science, catalysis, biology and medicine because of their chemical, structural and electronic versatility [1–4]. One of the most important properties of polyoxometalate anions is their ability to accept various numbers of electrons giving rise to mixed-valence species such as heteropolyblues and heteropolybrowns. In order to take advantage of their specific properties in solution, there has been much exploitation of the attachment of heteropolyanions (HPA) onto different substrates using different methods such as electrodeposition [5–9], adsorption [10–12] and HPA as the dopant immobilized into a polymer matrix [13–27]. These electrode coating techniques usually produce random spatial and orientational arrangements of the redox species in the film. Recently, Ingersoll et al. [28] and Sun et al. [29] produced multilayer films by alternating deposition. Clemente-Leon et al. [30] prepared an ultrathin film containing HPA by using the Langmuir–Blodgett (LB) technique. These experimental techniques can organize molecular assemblies with a precise control of layer composition and thickness. Heteropolyanions have also been used in the formation of self-assembled monolayers of Keggin HPAs [31] and in heterogeneous electrocatalysis using Anderson–Perlof HPAs [32]. More recently, the electrochemistry [33] and the electrodeposition [34] of Anderson–Perlof HPAs have been reported.

In this communication, the main interest is to investigate the voltammetric response and the film formation of heteropolyoxometalates (HPOM) containing copper onto highly oriented pyrolytic graphite (HOPG) electrode surfaces by using cyclic voltammetry and *in situ* AFM.

2. Experimental details

The HPOMs $(NH_4)_3[RhMo_6O_{18}(OH)_6] \cdot 7\ H_2O$, HPOM (**1**), Cu(II)$NH_4[RhMo_6O_{18}(OH)_6] \cdot 7\ H_2O$, HPOM (**2**) and Cu(II)$NH_4[CoMo_6O_{18}(OH)_6] \cdot 7\ H_2O$, HPOM (**3**), were synthesized by Holguin [35] in agreement with the Ivanov–Emin technique [36]. The compounds were characterized by u.v.–vis., i.r. and X-ray powder diffraction methods. The electrochemical deposition was studied *in situ* with a NanoScope IIIa microscope (Digital Instruments, Sta. Barbara, CA). Electrochemical atomic force microscopy (EC-AFM), which combines a fluid cell under the control of a potentiostat and normal AFM imaging, were employed. For this study, HOPG was used as a working electrode, platinum wire as a counter electrode and silver wire as a pseudo-reference electrode. It is important to mention that the Ag wire is the most used pseudo-reference electrode for *in situ* EC-AFM experiments since the design and the geometry of the electrochemical cell do not allow the use of other common reference electrodes such as Ag/AgCl.

The difference between the Ag and the Ag/AgCl reference electrode is less than 100 mV.

Experiments were carried out at the solid–liquid interface at room temperature for HPOM concentrations of about 5.2×10^{-3} M. For all electrochemical studies a 0.1 M $LiClO_4$ solution was used as supporting electrolyte. Finally, AFM images were taken at open circuit in the contact mode with low scanning forces (0.3 N m^{-1}).

3. Results and discussion

Figure 1 shows the electrochemical response of the $(NH_4)_3[RhMo_6O_{18}(OH)_6] \cdot 7\ H_2O$, HPOM (**1**) in a $LiClO_4$ solution. In this case, no cathodic peak is observed but the current at the cathodic potential limit increases with the number of potential scan cycles (PSC), which is characteristic of HPA electrodeposition [34].

In Figure 2, a sequence of *in situ* AFM images shows the evolution of the electrodeposited film onto the HOPG surface as the number of PSC increased. Figure 2(a) presents a clean HOPG surface before electrodeposition. After 7 PSC, the AFM image (Figure 2(b)) shows some nodules randomly distributed over the surface. Finally, after 21 PSC, the number and size of the nodules has increased as shown in Figure 2(c). This behaviour clearly indicates that

Table 1. Maximum height (MH) and roughness values calculated on the AFM images for the HPOM electrodeposited films onto HOPG electrode surfaces against number of potential scan cycle

Compound	Number of cycles	Maximum height /nm	Roughness (RMS) /nm
HPA1	0/bare HOPG	6.2	2.2
	7	57.8	18.4
	14	163.4	55.3
HPA2	0/bare HOPG	11.8	7.7
	3	11.0	6.4
	7	6.4	6.1
	14	9.5	10.4
HPA3	0/bare HOPG	28.8	8.9
	1	25.1	14.6
	7	24.7	26.8
	14	23.9	29.3

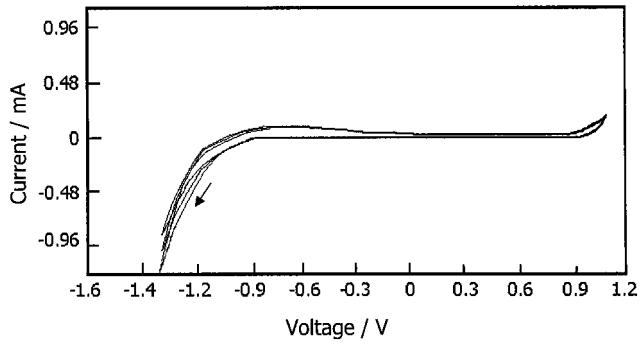

Fig. 1. Cyclic voltammogram of the $(NH_4)_3RhMo_6O_{18}(OH)_6] \cdot 7\ H_2O$ reduction at the HOPG electrode surface. HOPM 1 concentration was 5.12×10^{-3} M in a 0.1 M $LiClO_4$ solution. Scan rate $v = 0.075$ V s^{-1}.

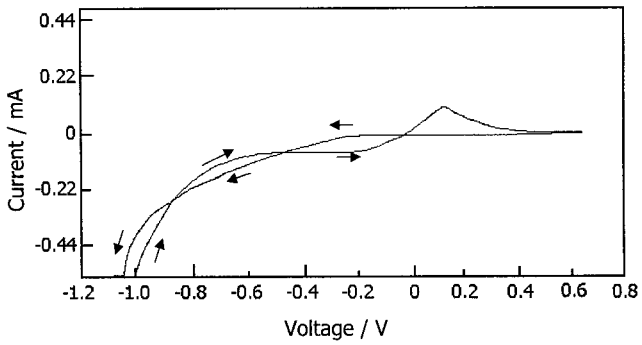

Fig. 3. Cyclic voltammogram of the HOPM 2 with Cu as a countercation at the HOPG electrode surface. HPOM 2 concentration was 5.12×10^{-3} M in a 0.1 M $LiClO_4$ solution. Scan rate $v = 0.075$ V s^{-1}.

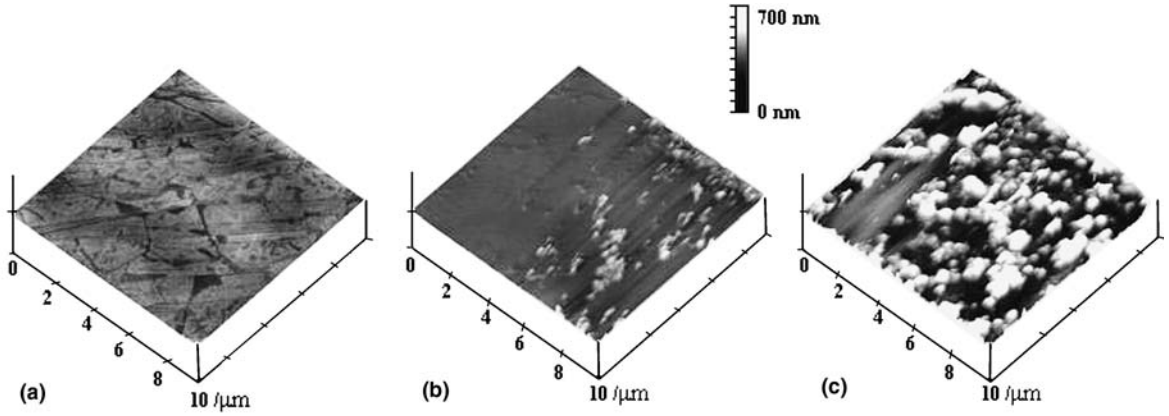

Fig. 2. Sequence of AFM images (10 × 10 μm) taken at the electrolyte–electrode interface onto the HOPG electrode surface after HPOM **1** electrodeposition. After: (a) none (bare HOPG), (b) three and (c) seven potential scan cycles. Vertical scale bar indicates height of surface features.

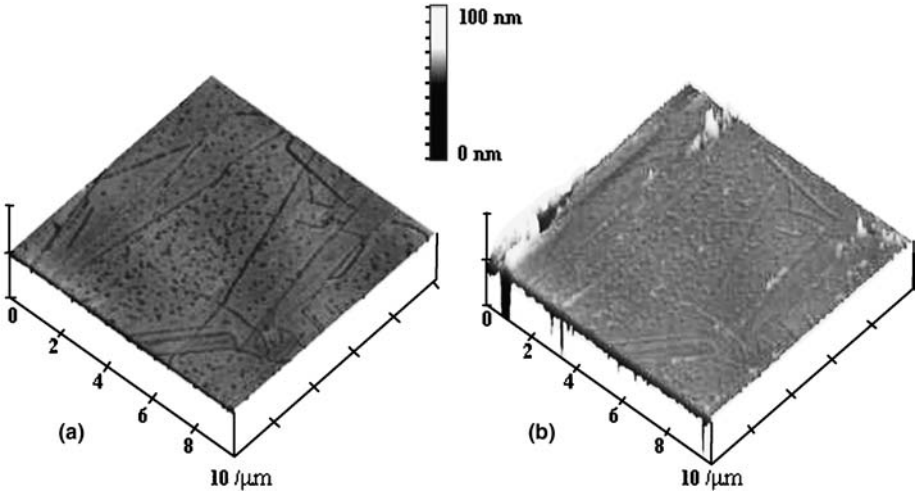

Fig. 4. 10×10 μm AFM images at the electrode–electrolyte interface after HPOM 2 electrodeposition. Images were taken after: (a) none (bare HOPG) and (b) three potential scan cycles. Vertical scale bar indicates height of surface features.

$[RhMo_6O_{18}\ (OH)_6]^{3-}$, HPA **1**, is being reduced and electrodeposited on the HOPG surface [34].

Figure 3 shows the electrochemical response of the $Cu(NH_4)[RhMo_6O_{18}(OH)_6] \cdot 7\ H_2O$, HPOM (**2**), on the HOPG electrode surface. This compound has Cu(II) as countercation in contrast with HPOM (**1**). Here, two main features can be observed. The first is the reduction of Cu(II) at −170 mV and the second is the reduction of $[RhMo_6O_{18}(OH)_6]^{3-}$ (HPA **2**) at −950 mV. Moreover, two potential cross links at −445 mV and −830 mV, which are characteristics of Cu(II) and HPA **2** nucleation and electrodeposition, respectively, are shown. The sequence of the electrodeposits can be seen in Figure 4: (a) shows a bare HOPG surface where some natural defects (holes and lines) are observed; (b) shows a HOPG surface covered with the electroreduced species (copper and HPA **2)** observed after 3 PSC. It is clear that a very thin film covers the electrode surface since the original holes and lines are still visible although the texture of the surface changed. A similar phenomenon was observed for another HPA [34].

Figure 5 shows the electrochemical behaviour of the $Cu(II)NH_4[CoMo_6O_{18}(OH)_6] \cdot 7\ H_2O$, HPOM **3**, on the HOPG electrode surface. HPOM **3** dissociates in Cu(II) and HPA **3** ($[CoMo_6O_{18}(OH)_6]^{3-}$) chemical species after it is mixed with the aqueous solution of the supporting electrolyte. In this case, the cathodic potential limit of about −1.1 V vs Ag wire, was only enough to allow copper reduction. This behaviour is very similar to that presented by Grujicic and Pesic for Cu electrodeposition onto a glassy carbon [37]. The cross-link of anodic to cathodic current at −493 mV suggests that the Cu electrodeposition occurs at the HOPG from the beginning of the redox process. After the cathodic potential limit was increased to a more negative value (−1.78 V), the electrodeposition of both, Cu and HPA 3, occurred as shown in Figure 6. In this voltammogram, an increase in the cathodic potential is observed. Moreover,

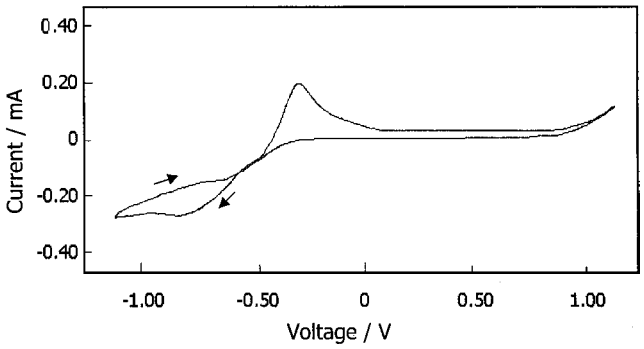

Fig. 5. Cyclic voltammogram of the HPOM 3 reduction with Cu as countercation. HPOM 3 concentration was 5.2×10^{-3} M in a 0.1 M $LiClO_4$ solution. Scan rate $v = 0.075$ V s^{-1}.

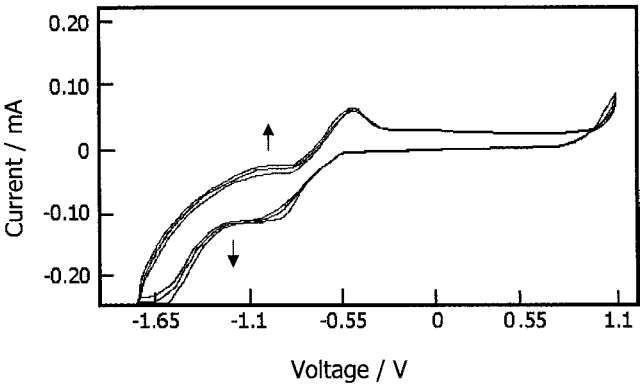

Fig. 6. Cyclic voltammogram showing seven consecutives cycles (reaching an $E_\lambda = -1.78$ V) of the HPOM 3 electrodeposition at the HOPG electrode surface. Concentrations as in Figure 5.

an anodic peak appears at −1.07 V which corresponds to $[CoMo_6O_{18}(OH)_6]^{3-}$ (HPA **3**) reduction and partial reoxidation (none-reversible). Although the anodic peak is not evident in the first cycle, its peak value increases as

the PSC does, which indicates that film formation is taking place as previously discussed [34]. Although the chemical form of the HPA3 electroreduced species (ERS-HPA **3**) is not known, it was demonstrated that the same complex, in the absence of Cu, produced a film which contained Co and Mo chemical species (EDS analysis) [34]. Therefore, from these results, the presence of Co, Mo and Cu species in the HPOM **3** film is inferred.

On the other hand, we know that copper electrodeposition is reversible in the absence of HPOM [37]. Furthermore, we know that the HPA **3** species is electrochemically irreversible in the absence of Cu(II) [34]. When we combine both species, the electrochemical reduction of Cu(II) also becomes irreversible, as can be seen from the plots. One possible explanation of this phenomenon is related to the processes taking place at the HOPG/solution interface. When the ERS-HPA **3** forms a film at the HOPG surface, Cu(II) reduces to Cu(0) and is trapped in the new film. As the number of PSC increases, the concentration of Cu at the interface decreases since the cathodic and anodic peak currents of copper decrease in contrast to those of HPA **3.** Thus, the electrodeposition and film formation of the ERS-HPA **3** modifies the electrochemical and chemical reversibility of Cu(II).

Since most of the time the electrodeposited films are very thin, it is very difficult to detect or measure the thickness of the new materials. Therefore, a roughness analysis (statistical measurement of the surface morphology) and a cross section study (vertical distance between the highest and lowest point in the image) of the electrode surface are required in order to show how the surface is modified by the presence of the electroreduced species. Therefore, a roughness analysis and a cross section study were performed on the AFM images for the three compounds under study. For the HPOM 1 complex, root mean square (RMS) analysis reveals the formation of a film on the HOPG surface. As the number of PSC increased, the size of the clusters and the average roughness values increased as a consequence of the surface modification. In contrast, HPOM **2** behaviour was different compared to the two other cases since the maximum height (MH) and the RMS roughness values initially decreased, indicating that the new film covered some natural defects of the HOPG making it smoother. However, after the 14th PSC, there was a MH and RMS roughness augmentation, which suggests that once the surface is uniform the film grows in a manner similar to HPOM **1**. Finally, the HPOM **3** complex shows roughness values that increase as the number of PSC increase while the opposite happens for the MH values. This can be explained in terms of surface modification. As new material is electrodeposited on the electrode, some of it goes to the natural defects of the substrate decreasing the MH but, at the same time, flat terraces of the surface are covered with small clusters which increase the average roughness value. An important difference among the films is that the complex without copper (HPOM **1**) forms a less smooth film, which can be important if a smooth texture is required. Finally, the small thickness values (nanometers) indicate the formation of thin films in all cases.

4. Conclusions

It was demonstrated by *in situ* AFM that, after reduction of HPAs of type $[MMo_6O_{18}(OH)_6]^{3-}$ with M = Rh(III) and Co(III) with Cu(II) as countercation, the HPA and Cu can be coelectrodeposited on the HOPG electrode surface using cyclic voltammetry. It is interesting to note that, although the chemical reduction and electrodeposition of copper is reversible in the absence of any HPOM complex, it turns irreversible when they are combined.

The HPOM **1** species, in the absence of copper, produced thick films in comparison with the other two compounds at the HOPG electrode surface with nodules of high size and high roughness values. In contrast, when copper is present as countercation, HPOM **2** and HPOM **3** species, thin films were observed at the HOPG electrode surface with nodules of small size and low roughness values. From these results, the modification of electrode surfaces with these compounds can be controlled in order to obtain a particular film texture with specific physical or chemical properties. Finally, by using this technique some metallic species can be trapped in inorganic films (previously characterized) in order to modify the film properties such as conductivity and porosity, among others. These experiments can be used in catalytic and electrocatalytic areas where specific surface properties are required.

Acknowledgements

The authors gratefully acknowledge Dr A. Moreno for the AFM equipment and facilities. This work had financial support by CONACyT, Project 36155-E.

References

1. M.T. Pope and A. Muller, *Angrew. Chem., Int. Ed. Engl.* **30** (1991) 34.
2. M.T. Pope, 'Heteropoly and Isopoly Oxometalates' (Springer-Verlag, Germany, 1983).
3. M.T. Pope and A. Muller, 'Polyoxometalates: from Platonic Solids to Antiretrovival Activity' (Kluwer, Dordrecht, 1994).
4. M. Misono, *Catal. Rev. Sci. Eng.* **29** (1987) 269.
5. B. Keita and L. Nadjo, *J. Electroanal. Chem.* **227** (1987) 1019.
6. B. Keita and L. Nadjo, *J. Electroanal. Chem.* **230** (1987) 85.
7. B. Keita and L. Nadjo, *J. Electroanal. Chem.* **243** (1988) 87.
8. B. Keita and L. Nadjo, *J. Electroanal. Chem.* **247** (1988) 157.
9. B. Keita and L. Nadjo, *J. Electroanal. Chem.* **354** (1993) 295.
10. S. Dong and B. Wang, *Electrochim. Acta* **37** (1992) 11.
11. B. Wang and S. Dong, *Electrochim. Acta* **37** (1992) 1859.
12. B. Wang and S. Dong, *J. Electroanal. Chem.* **328** (1992) 245.

13. G. Bidan, E.M. Genies and M. Lapkowski, *J. Electroanal. Chem.* **251** (1988) 297.
14. G. Bidan, E.M. Genies and M. Lapkowski, *Synth. Met.* **31** (1989) 327.
15. M. Lapkowski, G. Bidan and M. Fournier, *Synth. Met.* **41** (1991) 407.
16. G. Bidan, M. Lapkowski and J.P. Travers, *Synth. Met.* **28** (1989) 113.
17. B. Fabre, G. Bidan and M. Lapkowski, *J. Chem. Soc. Chem. Commun.* (1994) 1509.
18. S. Dong, F. Song, B. Wang and B. Liu, *Electroanalysis* **4** (1992) 643.
19. S. Dong, B. Wang and F. Song, *Chem. Lett.* **215** (1992) 414.
20. S. Dong and Z. Jin, *Chin. Chim. Acta* **47** (1989) 922.
21. S. Dong and W. Jin, *J. Electroanal. Chem.* **354** (1993) 87.
22. S. Dong and M. Liu, *Electrochim. Acta* **39** (1994) 947.
23. B. Keita, A. Belhouari, L. Nadjo and R. Contant, *J. Electroanal. Chem.* **381** (1995) 243.
24. B. Keita and L. Nadjo, *J. Electroanal. Chem.* **255** (1988) 303.
25. B. Keita, K. Essaadi and L. Nadjo, *J. Electroanal. Chem.* **259** (1989) 127.
26. B. Keita, A. Mahmoud and L. Nadjo, *J. Electroanal. Chem.* **386** (1995) 245.
27. H. Sung, H. So and W. Paik, *Electrochim. Acta* **39** (1994) 645.
28. D. Ingersoll, P.J. Kulesza and L.R. Faulkner, *J. Electrochem. Soc.* **140** (1994) 840.
29. C. Sun, J. Zhao, H. Xu, Y. Sun, X. Zhang and J. Shen, *J. Electroanal. Chem.* **435** (1997) 63.
30. M. Clemente-Leon, B. Agricole, C. Mingotand, C.J. Gomez-Garcia, E. Coronado and P. Delhaes, *Langmuir* **13** (1997) 2340.
31. S. Liu, Z. Tang, A. Bo, E. Wang and S. Dong, *J. Electroanal. Chem.* **458** (1998) 87.
32. T. Hernández-Pérez, S. Holguín and I. González, Proceedings of the 'Electro-chemicaly Deposited Thin Films' Symposium, 186th ESM, Miami Beach, USA (1995), p. 339.
33. A.L. Nolan, C.C. Allen, R.C. Burns, D.C. Craig and S. Lawrance, *Aust. J. Chem.* **51** (1998) 825.
34. M. Rivera, S. Holguín, A. Moreno, J.D. Sepúlveda-Sánchez and T. Hernández-Pérez, *J. Electrochem. Soc.* **149** (2002) E84.
35. S. Holguín, 'Synthesis and characterization of new heteropolyanions', Doctoral dissertation, Moscow, Russia (1978).
36. B.N. Ivanov'Emin and Y.I. Rabavik, *Zh. Neorg. Khim.* **3** (1958) 2449.
37. D. Grujicic and B. Pesic, *Electrochim. Acta* **47** (2002) 2901.